This paper was presented at the 1st International Conference on Large-Scale Grid Integration of Renewable Energy in India | New Delhi, India | 06-08 Sep., 2017

Fast frequency support from wind power plant

Harshank Agarwal and Zakir Rather
Department of Energy Science and Engineering
Indian Institute of Technology, Bombay
Mumbai, India

Abstract— **Wind Energy penetration has increased significantly over the past few decades, which has resulted in displacement of conventional power plants connected to the grid, reduced system inertia and diminished sources of the ancillary services. Impact of diminished rotating mass (inertia) and primary frequency reserve in the grid is being addressed by various system operators through fast frequency reserve. In this paper, modified IEC model of type-4B variable speed WTG including aerodynamic and pitch control model is developed. Fast frequency response control scheme including droop and inertia has been implemented. Low voltage ride through (LVRT) scheme as per the Indian grid code was also implemented. The proposed model was tested in IEEE 14-bus and 39-bus system at different wind penetration levels. Simulations were performed in DigSILENT power factory and results were observed for 3 cases, i.e. without control, with only inertial control and with both inertial and droop control. It was observed that the control scheme is successful in arresting the Rate of change of frequency (RoCoF) and improving the nadir frequency while ensuring quick initial recovery of frequency.**

Keywords- wind penetration, inertial and droop control, frequency response, variable speed WTG

I. INTRODUCTION

Increased climate concern and depleting fossil fuel resources has shifted the focus of generation to renewables, with wind and solar PV power being the front runners. Some countries are already experiencing a significant penetration of wind power with their electricity share in the range of 50% and instantaneous power penetration from wind surpassing even 100%. With large scale penetration of wind energy in the grid, conventional power plants are being displaced resulting in the removal of the ancillary control services that were provided by such plants. Hence, there is a growing interest to provide control features for wind turbine generators (WTGs) akin to conventional synchronous power plant for secure and stable grid operation [1]–[4]. Wind driven displacement of conventional power plant lead to low inertia systems due to decreased rotating mass connected to the grid [5]. Since Rate of Change of Frequency (RoCoF) and the nadir frequency, following a loss of an infeed depend on net system inertia, and therefore, high wind penetrated systems are more prone to frequency instability [6]–[8]. Hence, maintaining minimum system inertia for stable frequency operation is becoming a concern for transmission system operators (TSOs).

A study on the Irish power system carried by the Irish TSO (EirGrid) has concluded that the system will be insecure for around 30% of the year in 2020 due to insufficient system inertia [9]. Further, emerging issues with large-scale wind penetration such as a voltage dip induced frequency event, also weaken frequency stability of such grid [10]. To tackle these issue, TSOs are introducing a new ancillary service product known as 'Fast frequency response (FFR)' to supplement synchronous inertial response (SIR). FFR is faster than primary frequency reserve and run in conjunction with SIR. It is important to mention that FFR, which is combined inertial and fast droop response, is used in addition to regular frequency operating reserves. Various control techniques to emulate inertia from wind turbines have been suggested in the literature over the past years [1], [3], [4], [11], [12]. Conventional Synchronous generators increases or decreases the energy of the rotating masses as soon as it senses any change in frequency [1], [13]. However, variable speed wind turbines do not have any inherent frequency response. Further, unlike conventional generators, the fast frequency response of variable WTG is dependent on the local wind speed and hence cannot be quantitatively determined by the grid operators. Therefore, additional controls have to be employed to supply FFR reserve from WTGs during a frequency excursion in the grid.

FFR can be supplied by either utilizing available inertia and aerodynamic power at more than rated wind speed, or from available inertia and from the reserve margin in de-loaded WTGs at low wind speed [1]. Inertial control is the first control loop to be activated following a frequency event, with its response normally determined by RoCoF measured locally. Inertial control extracts energy stored in the rotating mass of the turbine thereby reducing the WTG speed. Droop control loop, on the other hand, depends on the change in frequency and extracts the available aerodynamic power. The active power output increase from a WTG during a frequency event may vary from system to system, however it is usually in between 5-10% of the rated WTG power [14].

. Any mismatch between generation and consumption leads to a frequency event which result in frequency deviation, depending on the magnitude of the mismatch and

the net system inertia [15]. The focus in this paper is to study FFR from Type 4 WTG system to support the grid frequency during a frequency event. The improvement in the frequency nadir and recovery at different penetration levels by employing the FFR control scheme in modified type 4b model wind turbine operated at below rated power has been presented. The rate of active power injection post fault is also regulated as a fast variations in active power injection may lead to mechanical stresses in the turbine rotor [16]. Section II describes modelling of WTGs along with the inertial and droop control adopted for WTGs for frequency support. The test systems used in this study are presented in Section III. Case study results and discussions are provided in Section IV followed by concluding remarks in Section V.

II. MODELLING OF FULL CONVERTER WIND TURBINE GENERATOR SYSTEM

The technology associated with wind turbine has evolved continuously. As the time has progressed, wind turbines have become more efficient and provide better control features. Presently, one of the main focus is to model a generic WTG that with maximum control features, which can work in any environment. In this work, Type 4B WTG model developed has been adopted from IEC model [17]. To make the model more generic and realistic, pitch control, aerodynamic power control, frequency control and LVRT protection blocks were added

A. Pitch control

Standard IEC type 4b model does not incorporate the pitch control block. However, to implement a more realistic and generic model for FFR application, pitch control block was integrated with the model. The pitch angle is used to control generator speed and aerodynamic torque when the available wind power exceeds the generator capacity. Pitch control limits the rate as well as the amplitude of the pitch angle. The rate of pitch angle variation has to be controlled as the pitch angle cannot be changed suddenly due to time constant of the servomechanism, and the mechanical stresses in the blade. The difference in the reference and the measured generator speed is fed into a PI controller which gives a reference value for the pitch angle as shown in Fig. 1. The implemented pitch control is given in (1)-(4) [18].

$$\frac{dx_p}{dt} = K_{iw}(\omega_{WTR} - \omega_{ref}) \quad (1)$$

$$\frac{dx_c}{dt} = K_{ic}(P_{ord} - P_{WTref}) \quad (2)$$

$$\frac{d\theta}{dt} = \frac{1}{T_{thet}}(\theta_{cmd} - \theta) \quad (3)$$

$$\theta_{cmd} = x_p + x_c + K_{pw}(\omega_{WTR} - \omega_{ref}) + K_{pc}(P_{ord} - P_{WTref}) \quad (4)$$

Where,

x_p is the integrator of the pitch controller,
x_c is the integrator of the pitch compensator,
K_{iw} is the integrator gain in pitch controller,
K_{pw} is the integrator gain in pitch compensator,
K_{pc} is the proportional gain in compensator,
θ_{cmd} is the summation of the aforementioned integrals,
P_{ord} and P_{WTref} are the measured and reference power respectively

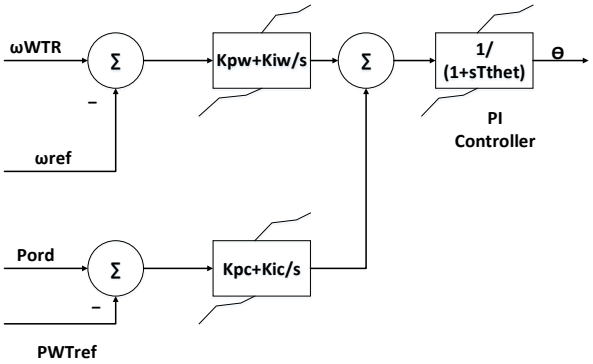

Figure 1. Pitch control

B. Frequency support strategy

The frequency support strategy used in this work comprises of both inertial and droop control as shown in Fig. 2. This frequency controller provides frequency response from WTG in case of a frequency excursion in the system. Inertial control is faster control which is activated as soon as RoCoF is detected. Droop control, on the other hand, is a slightly delayed response which acts for a prolonged period. Both the droop response and the inertial response signal is fed to the active power controller. The droop and inertial response is determined by (5) and (6) respectively.

$$Droop\ Response = (F_{meas} - F_{ref}) * K_{droop} \quad (5)$$

$$Inertial\ Response = \frac{dF_{meas}}{dt} * K_{inertial} \quad (6)$$

C. Active power control

The active power controller controls the active power output from the WTG. The initial set point of the active power (P_{ref}) is decided by the load flow conditions. This Power is divided by the measured voltage to calculate the active current set point (I_{pcmd}) to the generator. Fig. 3 shows the implemented power control block. In case of a fault, I_{pmax} signal is calculated using a current limiter block which restricts I_{pcmd} to a maximum permissible value during the fault. If a frequency fault occurs, the droop and the inertial parameters from the frequency block are added and subtracted respectively to adjust the active power setpoint. ω_{gen} is the generator speed which is used to calculate the generator torque.

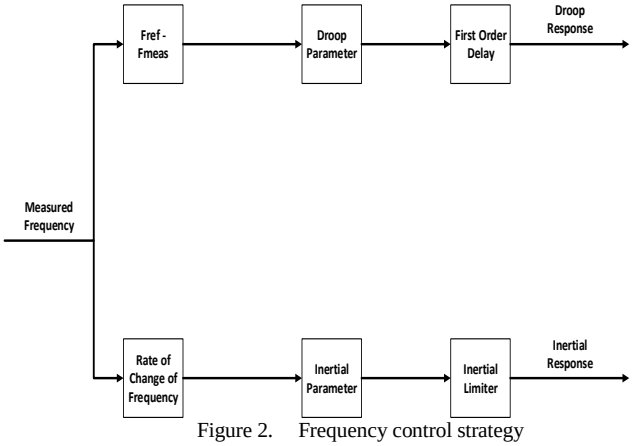

Figure 2. Frequency control strategy

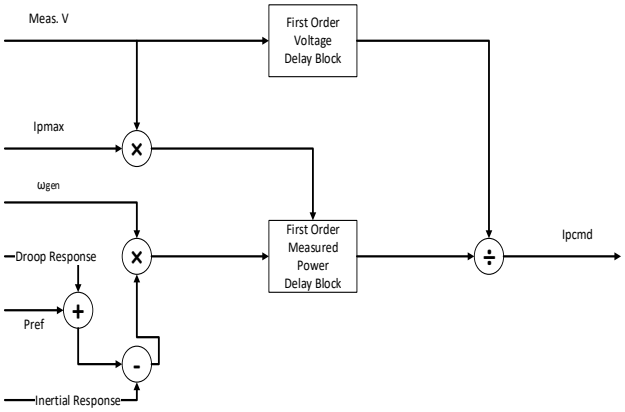

Figure 3. Active power control block

III. SYSTEM MODEL

To investigate frequency support from WTGs, two IEEE bench mark systems, IEEE 14 bus and IEEE 39 bus systems, which were modified to accommodate wind energy, have been developed in PowerFactory DigSILENT platform. The 14-bus system has 14 buses, 5 generators, 11 loads, 16 transmission lines, 5 transformers and one shunt capacitor. The nominal frequency of the system is 60 Hz. Three wind farms, Wind Farm 1, Wind Farm 2 and Wind Farm 3 of capacities 50, 100 and 100 MW were connected at bus 5, bus 13 and bus 4 respectively, as shown in Fig. 4.

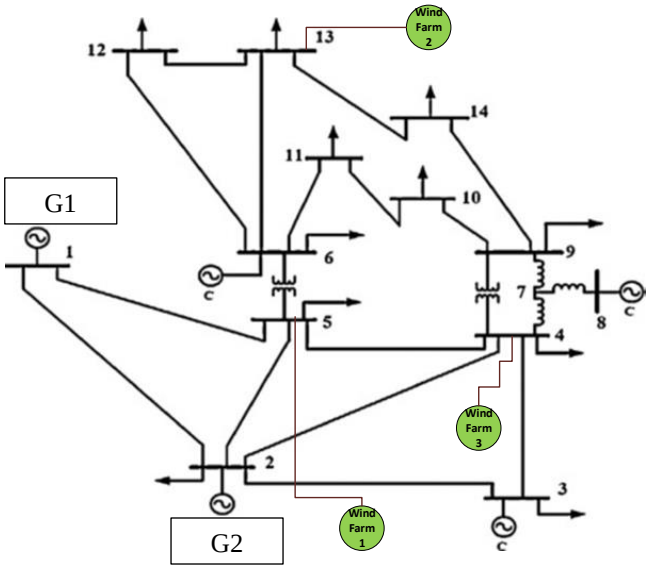

Figure 4. Modified 14-bus system

In addition to IEEE 14 bus system, IEEE 39 bus system which is relatively a larger system was also considered in the study. The 39 Bus New England System is a simplified model of the high voltage transmission system in the northeast of the U.S.A. The 39 Bus New England System consists of 39 buses (nodes), 10 generators, 19 loads, 34 lines and 12 transformers. The system works at a nominal frequency of 60 Hz and the mains nominal voltage level is 345 kV. A total of 7 wind farms operating at 80% of rated power were integrated with the 39-bus system. Fig. 5 shows the modified 39 bus system. Some of the conventional plants were not dispatched to accommodate wind power generation.

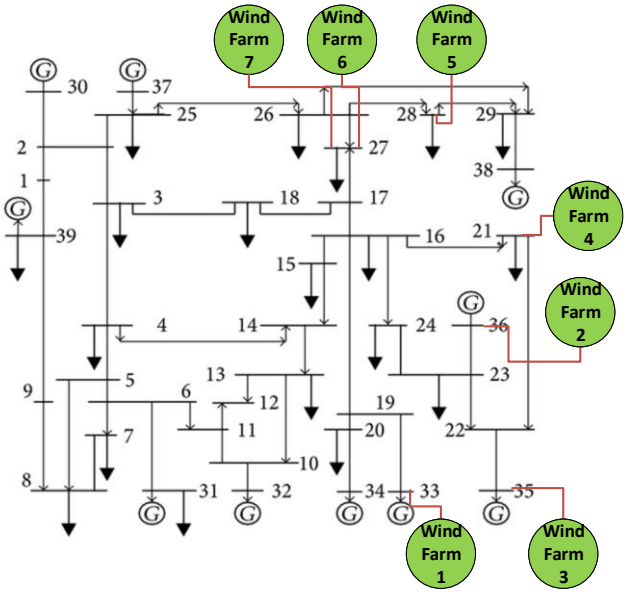

Figure 5. Modified 39-bus system

Table I shows the WTGs that were connected at different buses in the system.

TABLE I. WIND FARMS BUS NUMBER

Wind farm	Wind farm capacity (MW)	Bus Number
Wind farm 1	800	33
Wind farm 2	600	36
Wind farm 3	600	35
Wind farm 4	600	21
Wind farm 5	600	28
Wind farm 6	600	27
Wind farm 7	800	27

IV. RESULTS AND DISCUSSIONS

To observe the frequency of the entire system, centre of inertia (COI) frequency was calculated and plotted. The COI frequency is calculated using the aggregated swing's equation,

$$f_{COI} = \frac{\sum_{i=1}^{n} H_i S_i f_i}{\sum_{i=1}^{n} H_i S_i} \quad (7)$$

Where,
H_i is the inertia constant of the i^{th} generator
S_i is the rated power of the i^{th} generator and
f_i is frequency of i^{th} generator

A. 14-bus system

The aggregate capacity of the three connected Wind Farms is 250 MW. While the conventional power plant connected to bus 9 was not dispatched, the total wind power output of 200 MW amounted to 75% wind penetration level in the modified system. At such a higher wind penetration level, frequency operating reserves were supplied from wind farms which were operated in de-loaded state. Table II shows

the load flow based active power generation that was observed from different wind farms.

TABLE II. MODIFIED 14-BUS GENERATION AT 75% PENETRATION

Generator	Bus Number	Active Power Output (MW)
G1	1	25.2
G2	2	40
Wind farm 1 (25 WTGs)	5	40
Wind farm 2 (50 WTGs)	13	80
Wind farm 3 (50 WTGs)	4	80
Total		**265.2**

An outage of wind farm 2 wind farm 2 was observed at t=10 s. The loss of wind generation results in the system frequency drop as can be seen from Fig. 6. The frequency nadir of 59 Hz is reached, while primary frequency reserve is supplied from conventional power plants. Both the droop control and inertial control of wind turbines were deactivated.

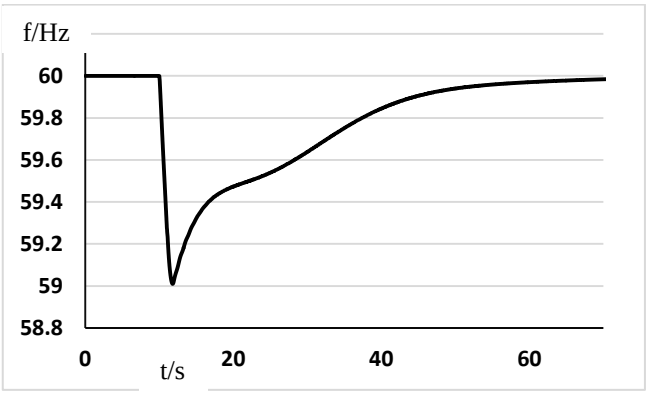

Figure 6. Frequency with no control from WTG

In the next case, for the same generation event, inertial control of wind turbine control was activated to study the effect of emulated inertial response from WTGs. It can be observed from Fig. 7, compared to the case shown in Fig. 7, there is an improved frequency response due to inertial response from WTGs. The nadir is improved from 59 Hz to 59.23 Hz, with an improvement of 0.23 Hz as compared to no control. The inertial response of wind farm1 is plotted in Fig. 8.

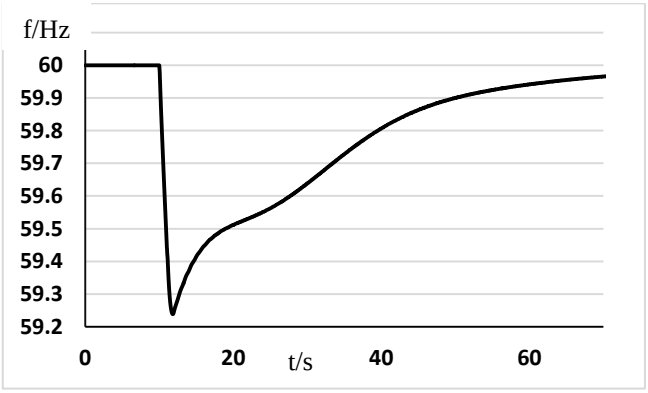

Figure 7. Frequency with inertial control from WTG

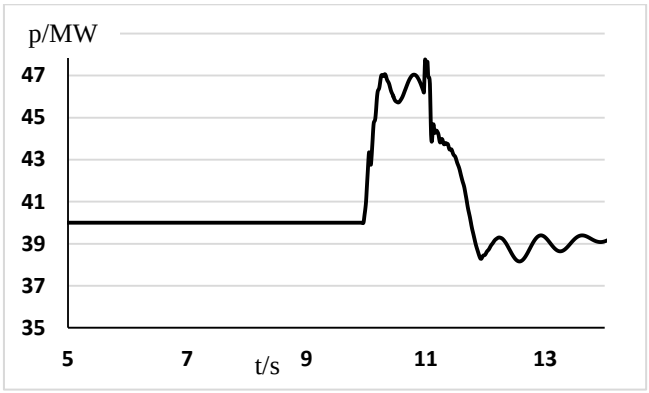

Figure 8. Active power output of wind farm 1

The additional energy released from WTG from the rotational energy results in WTG rotor speed reduction as shown in Fig. 9. The overproduction from a WTG is followed by an underproduction period along with the frequency recovery, as the WTGs try to regain their speed which leads to lower active power production, Fig. 8.

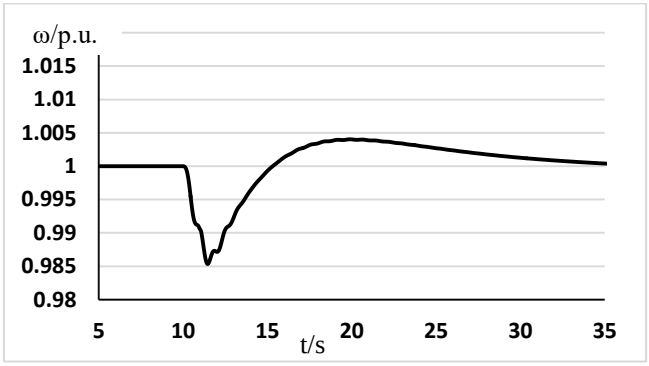

Figure 9. Wind farm 1 rotor speed

Finally, the system was run with both the droop and inertial control activated to study both the overall improvement in the system frequency response. As it can be observed from Fig. 10, there is a further improvement in the frequency nadir (59.42) point when both the controls are activated.

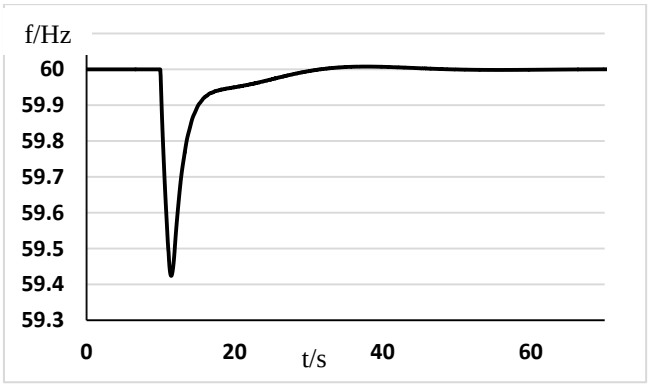

Figure 10. Both inertial and droop control from WTG

Fig. 11 shows frequency response in all the three cases, Case-I: without any frequency support from WTGs, Case-II: with inertial support from WTG, and Case-III: with both the inertial and droop response from WTGs. Besides improvement in frequency nadir, it can be observed that in

case-3, where WTGs provide both the inertial and primary frequency support, the recovery time is significantly improved. It is also important to observe that the recovery in case of inertial response is slightly delayed as compared to no frequency response from WTGs, which is due to energy recovery period by WTG following inertial response. The recovery rate of both droop and inertial control is the best of around 15s as compared to 40s when no frequency support from WTGs is employed.

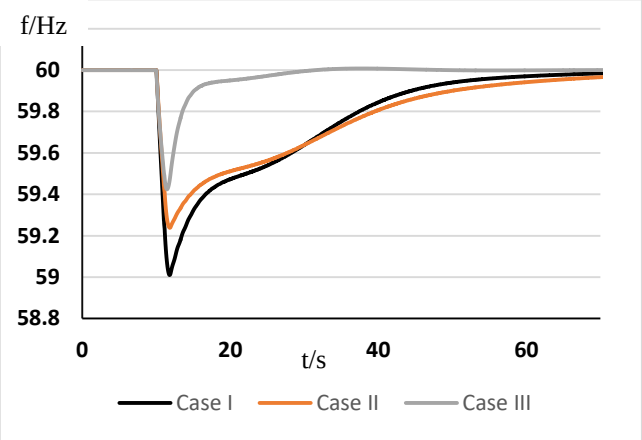

Figure 11. Frequency response in all 3 cases

B. 39-bus system

Similar fault conditions were simulated for the 39-bus system which is relatively a larger and a complex system. Table III shows the active power generation that was observed from different turbines on running the load flow conditions for 39-bus system at 25% penetration.

TABLE III. MODIFIED 39-BUS GENERATION AT 25% PENETRATION

Generator	Bus Number	Active Power Output (MW)
G 01	39	900
G 03	32	550
G 04	33	482
G 05	34	600
G 06	35	550
G 07	36	Shut Down
G 08	37	400
G 09	38	800
G 10	30	450
Wind Farm 1 (400 parallel WTGs)	33	Shut Down
Wind Farm 2 (300 parallel WTGs)	36	480
Wind Farm 3 (300 parallel WTGs)	35	Shut Down
Wind Farm 4 (300 parallel WTGs)	21	Shut Down
Wind Farm 5 (300 parallel WTGs)	28	480
Wind Farm 6 (300 parallel WTGs)	27	Shut Down
Wind Farm 7 (400 parallel WTGs)	27	640
Total		**6332**

A generation outage was simulated at 5s and reconnected at 5.3s. The frequency response in all the three cases is shown in Fig. 12, where it can be observed that frequency nadir without any WTG frequency support is around 59.67 Hz which is improved to 59.77 Hz when combined droop and inertial control is employed. The recovery periods follow the similar trend as that in the 14-bus system, with best recovery in case-3. Table IV shows the modified active power generation from all generators for a 60% penetration case.

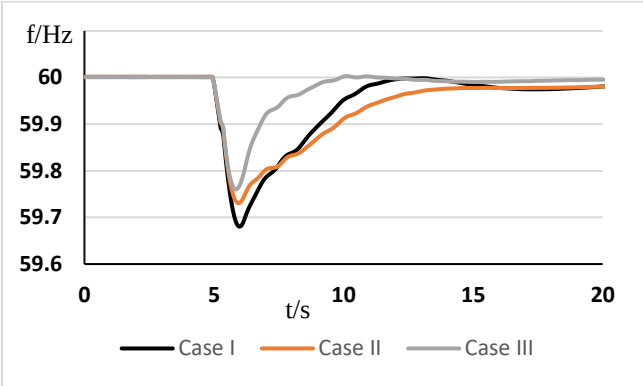

Figure 12: Frequency response in all 3 cases at 25% penetration

TABLE IV. MODIFIED 39-BUS GENERATION AT 60% PENETRATION

Generator	Bus Number	Active Power Output (MW)
G 01	39	650
G 02 (Reference Machine)	31	595
G 03	32	200
G 04	33	182
G 05	34	Shut Down
G 06	35	250
G 07	36	Shut Down
G 08	37	Shut Down
G 09	38	370
G 10	30	250
Wind Farm 1 (400 WTGs)	33	640
Wind Farm 2 (300 WTGs)	36	480
Wind Farm 3 (300 WTGs)	35	480
Wind Farm 4 (300 WTGs)	21	480
Wind Farm 5 (300 WTGs)	28	480
Wind Farm 6 (300 WTGs)	27	480
Wind Farm 7 (400 WTGs)	27	640
Total (MW)		**6177**

Frequency nadir is highest in the first case (59.18 Hz) which improves to 59.44 Hz with inertial control which can be seen in Fig. 13. The frequency further improves to 59.57 Hz when both controls are employed. Fig. 14 shows the aggregate active power generation from wind farms. It can be seen that during the fault, there is a shortfall of around 1100 MW. There is a higher total production during the fault and the recovery phase when frequency response is activated

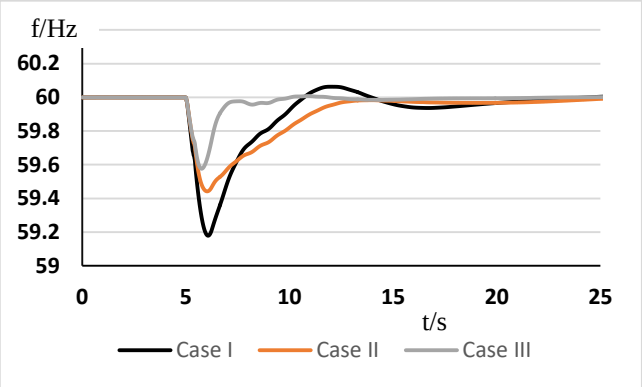

Figure 13. Frequency with all 3 cases at 60% penetration

as expected. There is a 10% increase in the active power production when only inertial control is activated and around 15% increase when both inertial and droop are activated.

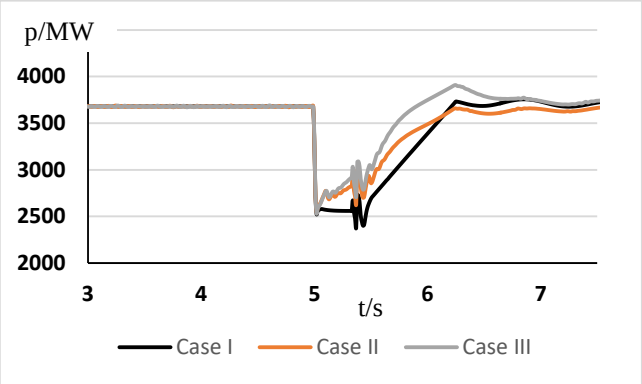

Figure 14. Total Wind generation in all 3 cases at 60% penetration

A case with wind penetration of 70% was also studies, details of which is provided in Table V.

TABLE V. MODIFIED 39-BUS GENERATION AT 70% PENETRATION

Generator	Bus Number	Active Power Output (MW)
G 01	39	300
G 02 (Reference Machine)	31	534
G 03	32	300
G 04	33	182
G 05	34	Shut Down
G 06	35	148
G 07	36	Shut Down
G 08	37	Shut Down
G 09	38	170
G 10	30	250
Wind Farm 1 (400 WTGs)	33	640
Wind Farm 2 (300 WTGs)	36	480
Wind Farm 3 (400 WTGs)	35	640
Wind Farm 4 (400 WTGs)	21	640
Wind Farm 5 (400 WTGs)	28	640
Wind Farm 6 (400 WTGs)	27	640
Wind Farm 7 (400 WTGs)	27	640
Total		**6204**

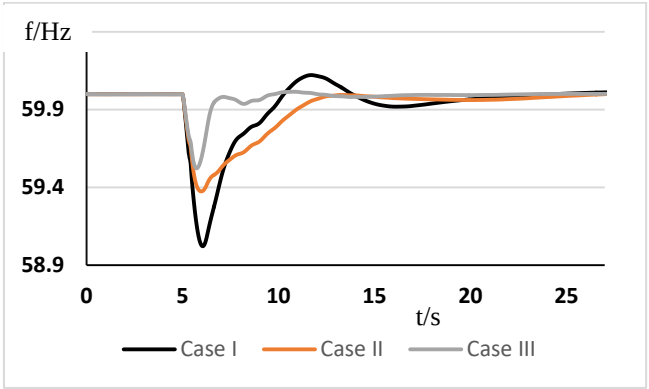

Figure 15. Frequency response for all 3 cases at 70% penetration

This caused an outage of around 1280 MW during the fault. For the 70% penetration case, Fig. 15 shows the response in all 3 cases. Trend similar to that in other lower penetration levels discussed, were observed. Fig. 18 plots the frequency nadir at different penetration levels the case when no frequency control by wind is activated. It can be seen that with increasing penetration levels, the nadir point also increases due to a larger outage of active power. The nadir is highest (59 Hz) in case of 70% penetration of wind and the lowest with 25% penetration (59.7 Hz).

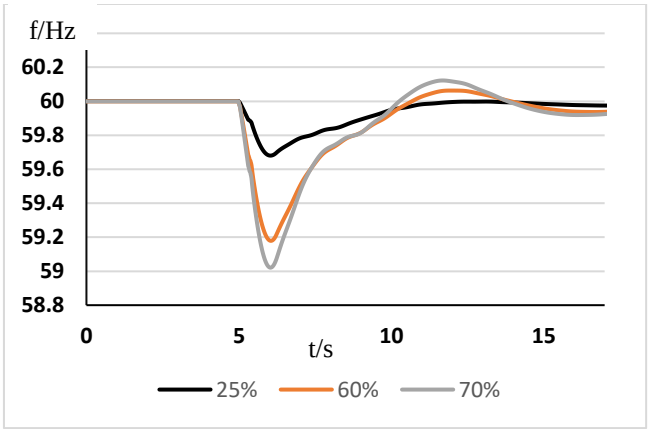

Figure 18. Nadir Point comparison at different penetration

V. CONCLUSIONS

In this paper fast frequency support from Type 4 based wind farms has been presented. Both the inertial and droop control loops were implemented. The aerodynamics and the mechanical mass were modeled in the type 4 wind turbine model, for realistic dynamic response during inertial and droop response. The frequency support from WTG was implemented in modified IEEE 14 bus and IEEE 39 bus system at various penetration levels. While it was observed that inertial response improves the nadir, the frequency recovery was deteriorated due to energy recovery by WTG following inertial response. The frequency response was best observed in case 3 where both the inertial and droop response were employed.

ACKNOWLEDGMENT

The authors are grateful to SERB/DST for the support through the project ECR/2016/001465 “Secure and Stable Grid Integration of Large-scale Wind Energy”. The authors

would also like to thank DigSILENT for providing the PowerFactory software for this research work.

REFERENCES

[1] J. Licari, J. Ekanayake, and I. Moore, "Inertia response from full-power converter-based permanent magnet wind generators," *J. Mod. Power Syst. Clean Energy*, vol. 1, no. 1, pp. 26–33, 2013.

[2] E. Muljadi, V. Gevorgian, and M. Singh, "Understanding Inertial and Frequency Response of Wind Power Plants Preprint," *2012 IEEE Power Electronics and Machines in Wind Applications (PEMWA)*, no. July. pp. 1–8, 2012.

[3] J. F. Conroy and R. Watson, "Frequency response capability of full converter wind turbine generators in comparison to conventional generation," *IEEE Trans. Power Syst.*, vol. 23, no. 2, pp. 649–656, 2008.

[4] J. Morren, S. Member, S. W. H. De Haan, W. L. Kling, and J. A. Ferreira, "Wind Turbines Emulating Inertia and Supporting Primary Frequency Control," *IEEE Trans. POWER Syst.*, vol. 21, no. 1, pp. 2005–2006, 2006.

[5] L. Ruttledge and D. Flynn, "Emulated inertial response from wind turbines: Gain scheduling and resource coordination," *IEEE Trans. Power Syst.*, vol. 31, no. 5, pp. 3747–3755, 2016.

[6] F. M. Gonzalez-Longatt, "Impact of emulated inertia from wind power on under-frequency protection schemes of future power systems," *J. Mod. Power Syst. Clean Energy*, vol. 4, no. 2, pp. 211–218, 2016.

[7] A. Ulbig, T. S. Borsche, and G. Andersson, "Impact of Low Rotational Inertia on Power System Stability and Operation," *IFAC World Congress*. Capetown, pp. 1–12, 2014.

[8] I. A. Gowaid, A. El-Zawawi, and M. El-Gammal, "Improved inertia and frequency support from grid-connected DFIG wind farms," *2011 IEEE/PES Power Systems Conference and Exposition, PSCE 2011*. IEEE, Phoenix, AZ, USA, 2011.

[9] D. Flynn *et al.*, "Technical impacts of high penetration levels of wind power on power system stability," *Wiley Interdiscip. Rev. Energy Environ.*, vol. 6, no. 2, pp. 1–19, 2017.

[10] Z. Rather and D. Flynn, "Impact of voltage dip induced delayed active power recovery on wind integrated power systems," *Control Eng. Pract.*, vol. 61, pp. 124–133, 2017.

[11] L. Holdsworth, J. B. Ekanayake, and N. Jenkins, "Power system frequency response from fixed speed and doubly fed induction generator-based wind turbines," *Wind Energy*, vol. 7, no. 1, pp. 21–35, 2004.

[12] K. V. Vidyanandan and N. Senroy, "Primary Frequency Regulation by Deloaded Wind Turbines Using Variable Droop," *IEEE Trans. Power Syst.*, vol. 28, no. 2, pp. 1–1, 2012.

[13] I. Erlich and M. Wilch, "Primary frequency control by wind turbines," *Power and Energy Society General Meeting, 2010 IEEE*. IEEE, pp. 1–8, 2010.

[14] L. Ruttledge, J. O. Sullivan, N. Miller, and D. Flynn, "Frequency response of power systems with variable speed wind turbines," *IEEE Trans. Sustain. ENERGY*, vol. 3, no. 4, p. 4799, 2013.

[15] J. Aho, A. Buckspan, and J. H. Laks, "A tutorial of wind turbine control for supporting grid frequency through active power control," *Proc. of the American Control Conference*, no. March. pp. 3120–3131, 2012.

[16] Y. Wang, G. Delille, H. Bayem, X. Guillaud, B. Francois, and S. Member, "High Wind Power Penetration in Isolated Power Systems — Assessment of Wind Inertial and Primary Frequency Responses," *IEEE Trans. POWER Syst.*, vol. 28, no. 3, pp. 2412–2420, 2013.

[17] IEC 61400-27-1 (2015). Wind turbines Part 27-1: Electrical simulation models of wind turbines.

[18] Z. Dai, "Generic Wind Turbine Generator Model Comparison based on Optimal Parameter Fitting," University of Toronto, Toronto, 2014.